



HAL
open science

Revisiting the argmin direct control for the Cascaded H-Bridge Inverter

Manon Doré, Yassine Ariba, Oswaldo Lopez-Santos, Germain Garcia

► **To cite this version:**

Manon Doré, Yassine Ariba, Oswaldo Lopez-Santos, Germain Garcia. Revisiting the argmin direct control for the Cascaded H-Bridge Inverter. Conference on Control Technology and Applications CCTA 2024, Aug 2024, Newcastle upon Tyne, United Kingdom. hal-04627060v2

HAL Id: hal-04627060

<https://hal.science/hal-04627060v2>

Submitted on 2 Jul 2024

HAL is a multi-disciplinary open access archive for the deposit and dissemination of scientific research documents, whether they are published or not. The documents may come from teaching and research institutions in France or abroad, or from public or private research centers.

L'archive ouverte pluridisciplinaire **HAL**, est destinée au dépôt et à la diffusion de documents scientifiques de niveau recherche, publiés ou non, émanant des établissements d'enseignement et de recherche français ou étrangers, des laboratoires publics ou privés.

Revisiting the *argmin* direct control for the Cascaded H-Bridge Inverter

Manon Doré, Yassine Ariba, Oswaldo Lopez-Santos, and Germain Garcia

Abstract—This paper addresses the direct control of the Cascaded H-Bridge (CHB) converter as an inverter (DC-AC), using the *argmin* control law. This control law derived from the literature on switched affine systems has been used in the control community for direct control of DC-DC converters. However, it has limited effectiveness with the CHB, as it fails to take advantages of the modularity of this topology. To overcome this, a revisited *argmin* control law is proposed. This new version imposes extra constraints on control inputs to improve the tracking of a suitable reference, offering advantages over the classical *argmin* control law for this specific converter. Specifically, it significantly reduces switches commutations and the harmonic distortion. Results are further extended with a state feedback version to specify the closed-loop dynamic. All results are illustrated with simulations using PSIM.

I. INTRODUCTION

The Cascaded H-Bridge (CHB) Converter is a multilevel power converter employed as an inverter in high voltage or high power applications [1]. It finds application in various fields such as renewable energy systems [2], [3], electric vehicle propulsion [4], [5] and High Voltage Direct Current (HVDC) transmission [6], [7]. This converter produces high-quality voltage waveform, with reduced harmonic distortion and high efficiency [8]. The CHB inverter consists in multiple H-Bridges connected in series, also called cells. Each cell can be regarded as a module, making this converter topology highly modular and adaptable to different voltage levels. Additionally, its structure presents redundancy, providing fault tolerance capabilities [9].

From a modeling perspective, this converter’s model is linear, unlike other well known converters like the boost converter. Its specificity arises from the absence of energy storage elements within the circuit, meaning that the switches directly determine the output voltage level.

From a control perspective, converters are often considered as hybrid systems, specifically switched affine systems, exploiting the switching nature of transistors. Recent advances in control theory have introduced the so-called *argmin* control law for such systems [10], with several applications on converters [10]–[14]. In this paper, we point out that the *argmin* control law is inefficient for the CHB, and unable to take advantage of its modular topology. Instead of using the multilevel structure of the system, the control law naturally selects extreme output levels by optimization. This results in poor harmonic quality of the output and high switching losses.

M. Doré, Y. Ariba and G. Garcia are with LAAS-CNRS, Université de Toulouse, CNRS, INSA, Toulouse, France. Email: {mdore,yariba,garcia}@laas.fr. O. Lopez-Santos is with Departament d’Enginyeria Elèctrica, Electrònica i Automàtica, Universitat Rovira i Virgili, Tarragona, Spain. Email: oswaldo.lopez@urv.cat

To address this issue, this paper revisits the *argmin* control law so as to restore the benefit of the converter’s modularity. The asymptotic stability of the error origin (between the state and its reference) is proven using Lyapunov methodology for the closed-loop system. Results are extended with a state feedback version of the proposed control law, and simulations on PSIM illustrate the effectiveness of the approach.

II. MODELING

The circuit of the considered Cascaded H-Bridge inverter is shown in Figure 1. Each H-Bridge cell is fed by an isolated voltage source of same value, denoted V_{in} . According to the state of its switches, a cell can generate a constant voltage level: V_{in} , $-V_{in}$ or 0.

The states of the switches are represented by binary control variables denoted as u_i , where 0/1 correspond to open/close respectively, and $\bar{u}_i = 1 - u_i$. Each cell requires two control variables, such that the voltage between the arms of the i^{th} cell is $(u_{2i} - u_{2i-1})V_{in}$.

Each cell contributes to generate a portion of the overall output voltage V_{ond} . This voltage depends on the state of the switches, and takes values in the set $\{-mV_{in}; \dots; (m-1)V_{in}; mV_{in}\}$, where m is the number of cells. To complete the system, we consider that the converter is connected to a resistive load via an LC filter.

Considering the notations in Figure 1 and the series topology of the converter, Kirchoff’s laws allow to write the following model of the overall system:

$$\begin{cases} V_{ond} &= \sum_{i=1}^m (u_{2i} - u_{2i-1})V_{in} \\ (L_1 + L_2)\dot{i} &= V_{ond} - v_C \\ C\dot{v}_C &= i - \frac{v_C}{R} \\ y &= v_C \end{cases}$$

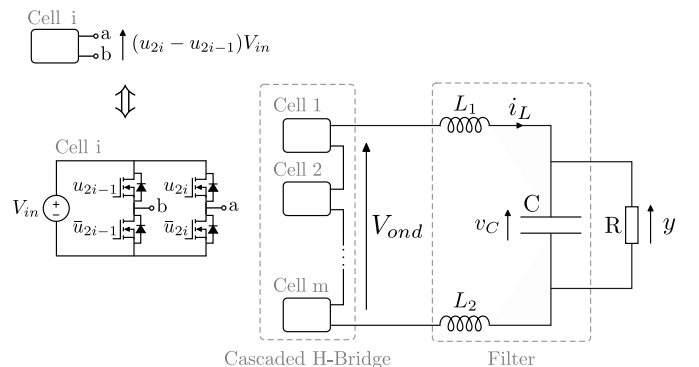


Fig. 1: System circuit

Taking $x = [i \ v_C]^T$ as a state vector, and defining $L := L_1 + L_2$, we can derive a state space model of the form:

$$\begin{cases} \dot{x} = A_0 x + \sum_{i=1}^{2m} u_i B_{u_i} V_{in} = A_0 x + B_0 V_{ond}(u) \\ y = C_0 x \end{cases}$$

where

$$A_0 = \begin{bmatrix} 0 & -\frac{1}{L} \\ \frac{1}{C} & -\frac{1}{RC} \end{bmatrix} \quad B_{u_i} = \begin{cases} \begin{bmatrix} -\frac{1}{L} \\ 0 \end{bmatrix} & \text{if } i \text{ is odd} \\ \begin{bmatrix} \frac{1}{L} \\ 0 \end{bmatrix} & \text{if } i \text{ is even} \end{cases}$$

$$B_0 = \begin{bmatrix} \frac{1}{L} \\ 0 \end{bmatrix} \quad C_0 = [0 \ 1] \quad u \in \{0; 1\}^{2m}$$

III. CONTROL

The objective of the control problem is to determine V_{ond} , through the control of the switches, such that the voltage y across the load tracks a sinusoidal reference waveform y_e to ensure the DC-AC function, such that

$$y_e = M \sin(\omega t) \quad (1)$$

Based on the circuit model, the current reference i_e associated to the output voltage reference (1) is:

$$i_e = C \dot{y}_e + \frac{y_e}{R} = CM\omega \cos(\omega t) + \frac{M}{R} \sin(\omega t) \quad (2)$$

And the reference V_{ond_e} of V_{ond} is:

$$\begin{aligned} V_{ond_e} &= L \dot{i}_e + y_e \\ &= M(1 - CL\omega^2) \sin(\omega t) + \frac{ML}{R} \omega \cos(\omega t) \end{aligned} \quad (3)$$

Remark 1: The time derivative of the state reference $x_e := \begin{bmatrix} i_e \\ y_e \end{bmatrix}$ is given by:

$$\begin{aligned} \dot{x}_e &= \begin{bmatrix} -CM\omega^2 \sin(\omega t) + \frac{M\omega}{R} \cos(\omega t) \\ M\omega \cos(\omega t) \end{bmatrix} = \begin{bmatrix} -\frac{y_e}{L} + \frac{V_{ond_e}}{L} \\ \frac{i_e}{C} - \frac{y_e}{RC} \end{bmatrix} \\ &= A_0 x_e + B_0 V_{ond_e} \end{aligned}$$

A given reference V_{ond_e} for V_{ond} must then ensure $V_{ond_e} \in [-mV_{in}, mV_{in}]$ to be admissible.

Each u_i variable can take value 0 or 1, resulting in 2^{2m} possible combinations. However, many combinations yield to the same V_{ond} voltage. Since V_{ond} can take only $2m + 1$ values, we need only one u_i combination for each voltage level to control the converter. For instance, in a CHB with 8 cells, there are 65536 combinations of u_i s, but only 17 of them are needed to generate every V_{ond} voltage level. To characterize control values, we define set U , composed of sets U_k that contains u_i s combinations, such that if $u \in U_k$, then $V_{ond}(u) = k \times V_{in}$, for $k \in \{-m, -m + 1, \dots, 0, 1, \dots, m\}$.

To propose a control law, we first introduce the following lemma, which provides a sufficient condition on V_{ond} to asymptotically stabilize the origin of the error signal.

Lemma 1: Let $e := x - x_e$ be the tracking error. For a given symmetric positive definite matrix $Q_C \in \mathbb{R}^{2 \times 2}$ and $P \in \mathbb{R}^{2 \times 2}$ satisfying the LMI

$$A_0^T P + P A_0 + 2Q_C < 0 \quad (4)$$

if $V_{ond}(u)$ is controlled such that $e^T P B_0 (V_{ond}(u) - V_{ond_e}) < 0$ always holds, then the origin of e is asymptotically stable, in the sense of Filippov.

Proof: Consider the Lyapunov function $V(e) = \frac{1}{2} e^T P e$ where $P = P^T > 0$ satisfies (4). V is clearly positive definite and radially unbounded. Its time derivative is

$$\dot{V}(e) = e^T P (A_0 e + B_0 (V_{ond}(u) - V_{ond_e}))$$

Considering inequality (4), we have

$$\dot{V}(e) \leq -e^T Q_C e + e^T P B_0 (V_{ond}(u) - V_{ond_e})$$

Therefore, if $e^T P B_0 (V_{ond}(u) - V_{ond_e}) \leq 0$, then $\dot{V}(e) < 0$ and the origin of e is asymptotically stable (AS). ■

Remark 2: For the considered CHB circuit, the matrix A_0 is Hurwitz, condition (4) is then always feasible.

In the following proposition, the classical *argmin* control law is recalled, with a slightly different proof though.

Proposition 1: Let the reference x_e be admissible. For P satisfying (4), the classical *argmin* control law

$$\begin{aligned} (u_1^*, \dots, u_{2m}^*) &= \underset{(d_1, \dots, d_{2m}) \in U}{\operatorname{argmin}} e^T P (A_0 x + B_0 V_{ond}(d)) \\ &= \underset{(d_1, \dots, d_{2m}) \in U}{\operatorname{argmin}} e^T P B_0 V_{ond}(d) \end{aligned} \quad (5)$$

asymptotically stabilize the origin of the tracking error e .

Proof: Considering the same Lyapunov function as in the proof of Lemma 1 and P satisfying (4), similar arguments leads to

$$\dot{V}(e) \leq e^T P B_0 (V_{ond}(u) - V_{ond_e})$$

By construction of the control law (5), the inequality

$$\min_{(u_1, \dots, u_{2m}) \in U} e^T P B_0 V_{ond}(u) \leq e^T P B_0 V_{ond_e}$$

holds, and leads to

$$e^T P B_0 (V_{ond}(u) - V_{ond_e}) \leq 0$$

Then, Lemma 1 is fulfilled and the origin of e is AS. ■

Lemma 1 shows that for given values of e , P and V_{ond_e} , multiple V_{ond} values can stabilize the origin of e , which give a certain degree of freedom in the control that can be exploited. The classical *argmin* control law can select many u_i combinations, but ends up selecting only extreme values, due to the optimisation mechanism. In Proposition 2, a reduced *argmin* control law is introduced. This new law uses the degree of freedom in the control to select V_{ond} values that are close to its reference V_{ond_e} . This is achieved by reducing the control values that the control law can select to those close to the reference V_{ond_e} .

Proposition 2: Let the reference x_e be admissible. For P satisfying (4), the reduced *argmin* control law

For $V_{ond_e} \in [kV_{in}, (k+1)V_{in}]$ then

$$(u_1^*, \dots, u_{2m}^*) = \underset{(d_1, \dots, d_{2m}) \in \{U_k, U_{k+1}\}}{\operatorname{argmin}} e^T P B_0 V_{ond}(d) \quad (6)$$

asymptotically stabilizes the origin of the tracking error e .

Proof: Considering the same Lyapunov function as in the proof of Lemma 1 and P satisfying (4), similar arguments leads to

$$\dot{V}(e) \leq e^T P B_0 (V_{ond}(u) - V_{ond_e})$$

The control law (6) can only select combinations in sets U_k or U_{k+1} as a control, leading to $V_{ond} = kV_{in}$ or $V_{ond} = (k+1)V_{in}$. By construction of the control law (6)

$$\min_{(u_1, \dots, u_{2m}) \in \{U_k, U_{k+1}\}} e^T P B_0 V_{ond}(u) < e^T P B_0 V_{ond_e}$$

, since $V_{ond_e} \in [kV_{in}, (k+1)V_{in}]$. Therefore, inequality

$$e^T P B_0 (V_{ond}(u) - V_{ond_e}) < 0$$

holds, Lemma 1 is fulfilled and the origin of e is AS. ■

IV. STATE FEEDBACK CONTROL

The proposed control strategy can be extended by including a state feedback in the control design. First, we study the dynamic of the tracking error $e = x - x_e$, where $x_e = [i_e \ y_e]^T$ is defined in (1) and (2). Its dynamic is

$$\dot{x}_e = A_0 x_e + B_0 V_{ond_e}$$

where V_{ond_e} from (3) is the reference of V_{ond} . The dynamic of the tracking error is

$$\dot{e} = \dot{x} - \dot{x}_e = A_0 e + B_0 (V_{ond}(u) - V_{ond_e})$$

Considering V_{ond} as a continuous virtual control, we design a state feedback control of the form:

$$V_{ond} = V_{ond_e} - K e$$

where the state feedback gain $K \in \mathbb{R}^{1 \times 2}$ has to be designed. The dynamic of the system would then be

$$\dot{e} = (A_0 - B_0 K) e := \bar{A} e$$

The gain K can be designed using the classical pole placement technique to achieve a desired performance of the closed-loop system.

Since V_{ond} is in fact discontinuous and takes a limited number of values, the key idea is to use the reduced version of the *argmin* control to ensure V_{ond} switches along the state feedback reference $V_C := V_{ond_e} - K e$.

Proposition 3: Let $e := x - x_e$ denote the tracking error, $K \in \mathbb{R}^{1 \times 2}$ a given state feedback gain ensuring the matrix $\bar{A} = A_0 - B_0 K$ is Hurwitz, and $V_C = V_{ond_e} - K e$ be an admissible state feedback reference. Let a given symmetric positive definite matrix $Q_C \in \mathbb{R}^{2 \times 2}$, and a symmetric positive definite matrix $P \in \mathbb{R}^{2 \times 2}$ solution of the LMI

$$\bar{A}^T P + P \bar{A} + 2Q_C < 0 \quad (7)$$

Then, the state feedback reduced *argmin* control law

For $V_C \in [kV_{in}, (k+1)V_{in}]$ then

$$(u_1^*, \dots, u_{2m}^*) = \underset{(d_1, \dots, d_{2m}) \in \{U_k, U_{k+1}\}}{\operatorname{argmin}} e^T P B_0 V_{ond}(d) \quad (8)$$

asymptotically stabilizes the origin of the tracking error e .

Proof: First, let's remark that the dynamic of the state reference can be expressed as:

$$\dot{x}_e = A_0 x_e + B_0 V_{ond_e} = A_0 x_e + B_0 (V_C + K e)$$

Then, consider the Lyapunov function $V(e) = \frac{1}{2} e^T P e$ where $P = P^T > 0$ satisfies (7). V is clearly positive definite and radially unbounded. Its time derivative is

$$\begin{aligned} \dot{V}(e) &= e^T P (A_0 x_e + B_0 V_{ond_e} - A_0 x_e - B_0 (V_C + K e)) \\ &= e^T P ((A_0 - B_0 K) e + B_0 (V_{ond_e} - V_C)) \end{aligned}$$

Considering LMI condition (7), we have

$$\dot{V}(e) \leq -e^T Q_C e + e^T P B_0 (V_{ond_e} - V_C) \leq e^T P B_0 (V_{ond_e} - V_C)$$

By construction of the control law (8), we have the following inequality

$$e^T P B_0 V_{ond_e} < e^T P B_0 V_C$$

involving

$$\dot{V}(e) \leq e^T P B_0 (V_{ond_e} - V_C) < 0$$

Since $\dot{V} < 0$, the origin of e is asymptotically stable. ■

Next, we will show through simulation of the application that using the specific control choice (6) reduces changes in state variables compared to using (5). It also reduces the number of switches commutations, which reduces the associated circuit losses. Additionally, less calculations are needed to establish the control, as the number of combinations to test is reduced from $2m + 1$ to 2. Moreover, the state-feedback extension allows to select the closed-loop dynamics of the tracking error.

V. SIMULATION

To illustrate the proposed control law, a CHB inverter with $m = 8$ H-Bridge cells is simulated with PSIM. The parameters of the circuit are given in Table I.

As explained in Section 3, first paragraph, we can use only one combination of u_i variables to generate each voltage level of V_{ond} . Table II presents sets U_k containing the u_i combination selected to obtain the 17 possible V_{ond} voltage levels. This specific choice ensure that when switching between two consecutive voltage levels, only one control variable, and thus two transistors, need to switch, which limits switching losses. For example, $u \in U_4 = (0, 0, 0, 0, 0, 0, 0, 0, 1, 0, 1, 0, 1, 0, 1)$ leads to $V_{ond} = 4V_{in}$. In this case, H-Bridges number 5, 6, 7 and 8 will each have a voltage equal to V_{in} between their arms.

For this example, the simulation step is $T_{int} = 1\mu s$ and the control update period is $T_{com} = 10\mu s$. The matrix P needed to compute the classic and reduced control laws (5) and (6) is obtain by solving (4) while minimizing the trace of P with MATLAB and a semidefinite programming (SDP) solver. For $Q_C = \begin{bmatrix} 1 & 0 \\ 0 & 10 \end{bmatrix}$ arbitrarily, we obtain $P = \begin{bmatrix} 0.2027 & -0.0002 \\ -0.0002 & 0.0223 \end{bmatrix}$.

To test the state feedback version, the gain K is designed to achieve a stable closed-loop dynamic with a damping coefficient of $\zeta = 1.1$ and a natural frequency $\omega_n = 4000 \text{ rad/s}$. The resulting gain is $K = [8.3455 \quad 2.1855]$. The matrix P

TABLE I: Circuit parameters

Parameter	Value	Parameter	Value
V_{in}	40 V	ω	$2\pi \times 50 \text{ rad/s}$
$L_1 = L_2$	1 mH	M	$220\sqrt{2} \text{ V}$
C	220 μF	R	10 Ω

TABLE II: Selected combinations of u_i to obtain all possible values of V_{ond}

U_i	V_{ond}	Active H-Bridge	u_i s equal to 1
8	8 V_{in}	1,2,3,4,5,6,7,8	2,4,6,8,10,12,14,16
7	7 V_{in}	2,3,4,5,6,7,8	4,6,8,10,12,14,16
6	6 V_{in}	3,4,5,6,7,8	6,8,10,12,14,16
5	5 V_{in}	4,5,6,7,8	8,10,12,14,16
4	4 V_{in}	5,6,7,8	10,12,14,16
3	3 V_{in}	6,7,8	12,14,16
2	2 V_{in}	7,8	14,16
1	V_{in}	8	16
0	0		
-1	-1 V_{in}	-1	1
-2	-2 V_{in}	-1,-2	1,3
-3	-3 V_{in}	-1,-2,-3	1,3,5
-4	-4 V_{in}	-1,-2,-3,-4	1,3,5,7
-5	-5 V_{in}	-1,-2,-3,-4,-5	1,3,5,7,9
-6	-6 V_{in}	-1,-2,-3,-4,-5,-6	1,3,5,7,9,11
-7	-7 V_{in}	-1,-2,-3,-4,-5,-6,-7	1,3,5,7,9,11,13
-8	-8 V_{in}	-1,-2,-3,-4,-5,-6,-7,-8	1,3,5,7,9,11,13,15

needed for this control law is computed for $Q_C = \begin{bmatrix} 1 & 0 \\ 0 & 10 \end{bmatrix}$.

We obtain $P = \begin{bmatrix} 0.0016 & 0.0027 \\ 0.0027 & 0.0061 \end{bmatrix}$ by minimizing its trace while solving (7) with MATLAB and a SDP solver.

Figure 2 presents the current with its reference for all control methods. The classical control results in larger high-frequency component, causing larger ripples. Like the output, the transient phase is longer with the reduced control than with the classical control, but it better tracks its reference, as emphasized in Figure 5b.

Figure 3 shows the evolution of the output voltage y compared to its reference for all control laws (m stands for milliseconds on the time axis). With the reduced *argmin* control, the output closely track its reference. The classical control produces a sinusoidal signal, but with a smaller amplitude than the reference, as depicted in Figure 5. This figure also pictures that the transient phase is longer with the reduced control, but the signal tracks its reference more accurately at steady state. A shorter transient is not surprising with the classical control, since it can select more negative values of the Lyapunov function's time derivative.

With the state-feedback control law, output and current follow their references after a short transient phase, with reduced oscillations. As depicted in Figure 6, signals reach their references faster with the state-feedback than with the reduced law without state-feedback. This is expected, as the state-feedback control law is tuned for a faster closed-loop system than the open-loop one.

To better understand the control behavior, Figure 4 shows the inverter output V_{ond} alongside its reference. The classic *argmin* control law selects only extreme V_{ond} values, due to the expression minimized by the law. The reduced version

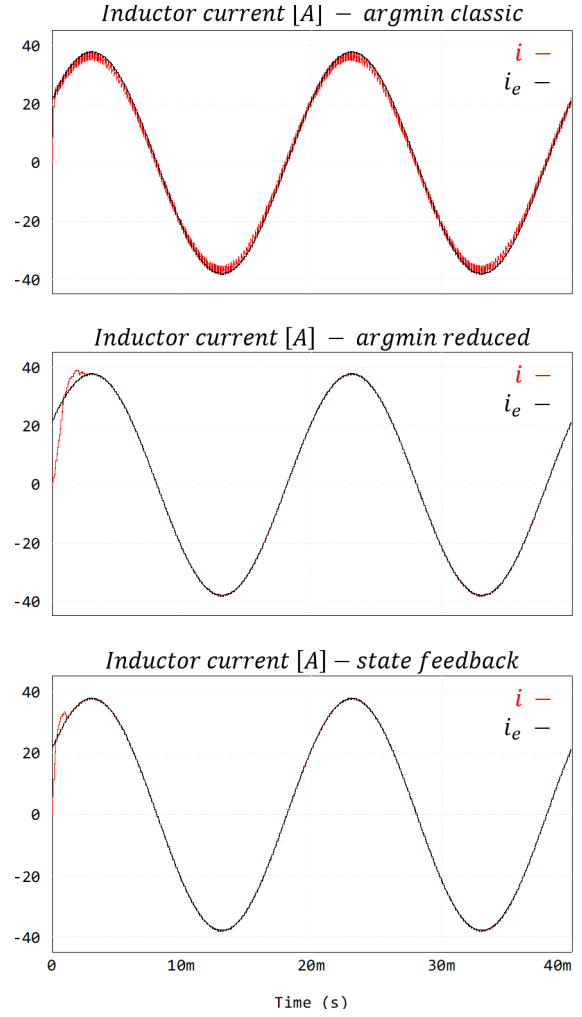


Fig. 2: Inductor current and reference for a: classical *argmin* - b: reduced *argmin* - c: state-feedback reduced *argmin*

(with or without state-feedback) forces to choose V_{ond} values close to its reference, ensuring accurate tracking, and reducing high-frequency content. The behavior of V_{ond} differs during the converter start-up, but is similar in the steady state for both reduced control laws. This is expected since $V_C = V_{ond_e}$ for $e = 0$, which is the case in steady-state.

Given the selected closed loop characteristic, we can also expect less overshoot with state-feedback in the system error compared to the reduced control law. This prediction is confirmed in Figure 7, which shows the output error for both control laws. It is clear that the transient phase is longer with the reduced control law (6).

Finally, Table III presents performance indicators for the output voltage with tested control laws. Indicators are: total number of commutation of u , mean tracking error and associated standard deviation computed over the last period of simulation (40 ms to 60 ms, representing steady-state), and THD (total harmonic distortion) computed over the last two simulation periods (20 ms to 60 ms). The reduced *argmin* control law significantly reduces the number of commutations, and thus associated losses compared to the

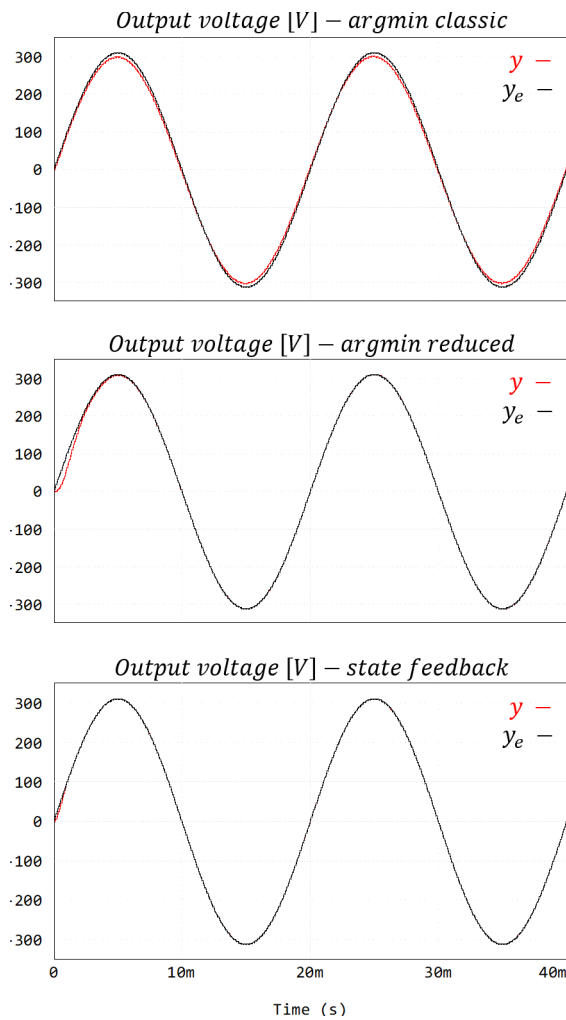


Fig. 3: Output voltage and reference for a: classical *argmin* - b: reduced *argmin* - c: state-feedback reduced *argmin*

TABLE III: Output voltage performance indicators

<i>argmin</i>	Total commut.	Mean error	Std. dev.	THD(%)
Classic (5)	39984	7.3170	3.6582	0.1231 %
Reduced (6)	3093	0.0530	0.0336	0.0165 %
State-feedback (8)	3397	0.0156	0.0109	0.0096 %

classic one. It also ensures better tracking and generates high-quality signal, with a THD around 0.01%. The state feedback version allows to select the behavior of the closed-loop system. As denoted on the figures, the system is faster and more precise with feedback. The overshoot is also reduced, but these improvements come at the cost of more switching, which is expected for faster dynamics.

VI. CONCLUSION

This paper has introduced a modified *argmin* control law designed for the cascaded H-Bridge inverter. Using a state space model of the system, we have derived reference signals for the inductor current and the capacitor voltage to achieve a sinusoidal output voltage. Through constraints on the admissible control inputs, we have significantly increased

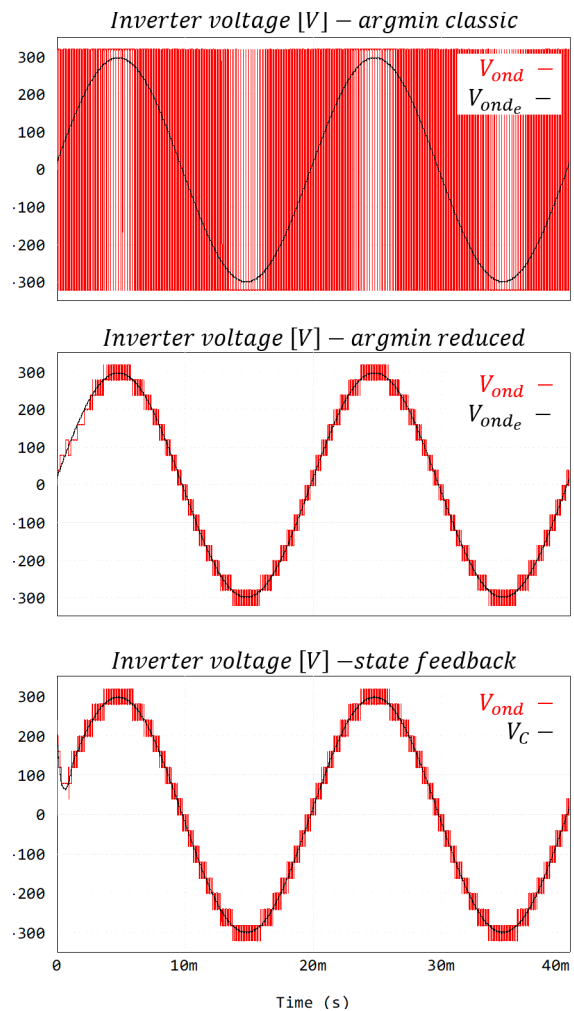


Fig. 4: Inverter output voltage and reference for a: classical *argmin* - b: reduced *argmin* - c: state-feedback reduced *argmin*

the output signal quality compared to the classic *argmin* control law, and reduced the number of commutations. We have also proposed a state feedback version of the reduced *argmin* control law, extending the approach, and simplifying the specification of the closed-loop dynamic. Simulations have shown that it was possible, for example, to speed up the system at the cost of increase the number of switch commutations.

However, some aspects were not addressed in the proposed approach. Specific circuit configuration choices were made to simplify the control problem, but alternative strategies could further reduce commutations and optimize power distribution among H-Bridge cells. Future research should focus on the robustness of the proposed strategy regarding external perturbations to give a more realistic study.

Also, a digital implementation of the proposed control in laboratory is being considered to further validate the concept and analyze the impact of delays, quantization and noise in the general performance of the system.

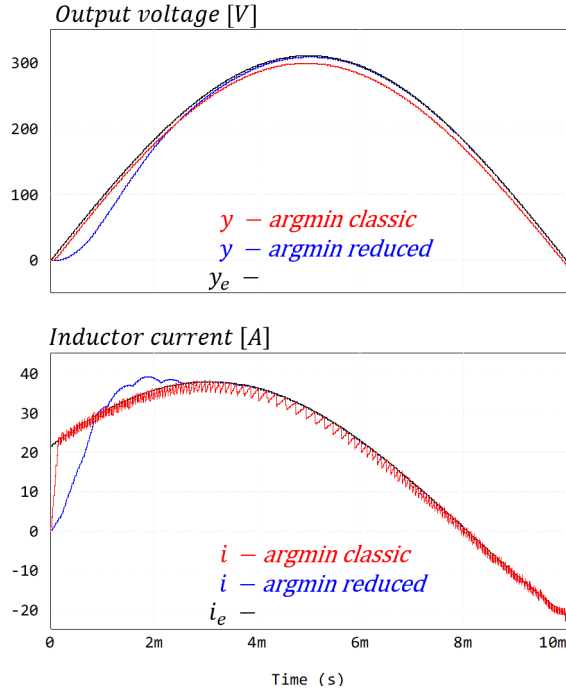


Fig. 5: Start-up of the converter for both control laws, a: output voltage - b: inductor current

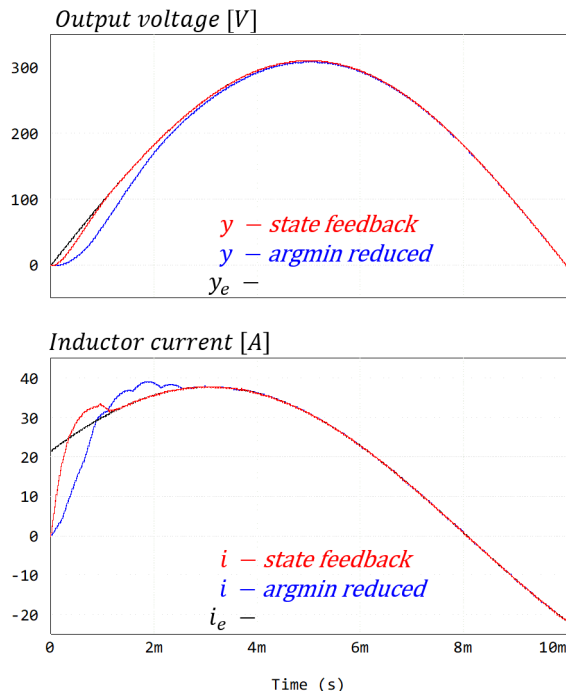


Fig. 6: Start-up of the converter for both control laws, a: output voltage - b: inductor current

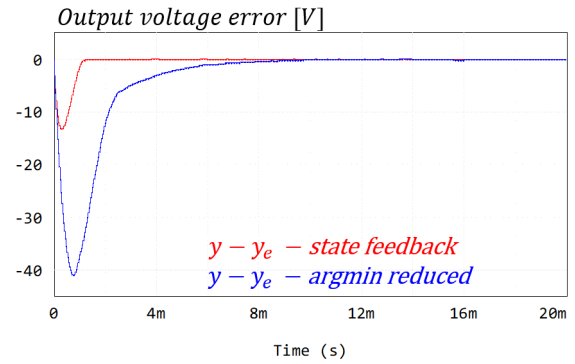


Fig. 7: Output voltage tracking error for both control laws

REFERENCES

- [1] L. G. Franquelo, J. Rodriguez, J. I. Leon, S. Kouro, R. Portillo, and M. A. Prats, "The age of multilevel converters arrives," *IEEE Industrial Electronics Magazine*, vol. 2, no. 2, pp. 28–39, June 2008, conference Name: IEEE Industrial Electronics Magazine.
- [2] Y. Yu, G. Konstantinou, B. Hredzak, and V. G. Agelidis, "Operation of cascaded h-bridge multilevel converters for large-scale photovoltaic power plants under bridge failures," *IEEE Transactions on Industrial Electronics*, vol. 62, no. 11, pp. 7228–7236, 2015.
- [3] B. Xiao, L. Hang, J. Mei, C. Riley, L. M. Tolbert, and B. Ozpineci, "Modular cascaded h-bridge multilevel pv inverter with distributed mppt for grid-connected applications," *IEEE Transactions on Industry Applications*, vol. 51, no. 2, pp. 1722–1731, 2015.
- [4] L. J. Kere, M. L. Doumbia, S. Kelouwani, and K. Agbossou, "Cascaded h-bridge multilevel converter for electric vehicle speed control," in *2015 IEEE Vehicle Power and Propulsion Conference (VPPC)*, 2015, pp. 1–6.
- [5] F. Khoucha, S. Lagoun, K. Marouani, A. Kheloui, and M. Benbouzid, "Hybrid cascaded h-bridge multilevel inverter motor drive dtc control for electric vehicles," in *2008 18th International Conference on Electrical Machines*, 2008, pp. 1–6.
- [6] Y. H. Liu, J. Arrillaga, and N. R. Watson, "Cascaded h-bridge voltage reinjection—part ii: Application to hvdc transmission," *IEEE Transactions on Power Delivery*, vol. 23, no. 2, pp. 1200–1206, 2008.
- [7] G. P. Adam, I. A. Abdelsalam, K. H. Ahmed, and B. W. Williams, "Hybrid multilevel converter with cascaded h-bridge cells for hvdc applications: Operating principle and scalability," *IEEE Transactions on Power Electronics*, vol. 30, no. 1, pp. 65–77, 2015.
- [8] J. Rodriguez, S. Bernet, B. Wu, J. O. Pontt, and S. Kouro, "Multilevel voltage-source-converter topologies for industrial medium-voltage drives," *IEEE Transactions on Industrial Electronics*, vol. 54, no. 6, pp. 2930–2945, 2007.
- [9] T. Wang, J. Zhang, H. Wang, Y. Wang, D. Diallo, and M. Benbouzid, "Multi-mode fault-tolerant control strategy for cascaded h-bridge multilevel inverters," *IET Power Electronics*, vol. 13, no. 14, pp. 3119–3126, 2020.
- [10] G. Deaecto, J. Geromel, F. Saldanha Garcia, and J. Pomilio, "Switched affine systems control design with application to DC-DC converters," *Control Theory & Applications, IET*, vol. 4, pp. 1201–1210, Aug. 2010.
- [11] C. Albea, G. Garcia, and L. Zaccarian, "Hybrid dynamic modeling and control of switched affine systems: Application to DC-DC converters," in *2015 54th IEEE Conference on Decision and Control (CDC)*, Dec. 2015, pp. 2264–2269.
- [12] G. Buneux, P. Riedinger, J. Daafouz, and L. Grimaud, "Adaptive stabilization of switched affine systems with unknown equilibrium points: Application to power converters," *Automatica*, vol. 99, pp. 82–91, Jan. 2019.
- [13] G. Garcia and O. Lopez Santos, "A Unified Approach for the Control of Power Electronics Converters. Part I—Stabilization and Regulation," *Applied Sciences*, vol. 11, no. 2, p. 631, Jan. 2021.
- [14] M. Doré, Y. Ariba, and G. Garcia, "Observer-based switched control of the three level neutral point clamped rectifier," in *2023 62nd IEEE Conference on Decision and Control (CDC)*, 2023, pp. 3580–3585.